Electronic Supplementary Material (ESI) for RSC Advances.

Supporting Information for Synergistic Effects of Halogen Bond and π-π Interactions in Thiophene-based Building Blocks

Jamey Wilson, Jon Steven Dal Williams, Chesney Petkovsek, Peyton Reves, Jonah W. Jurss, Nathan I. Hammer, Gregory Tschumper, Davita L. Watkins *

Department of Chemistry and Biochemistry, University of Mississippi, University, MS 38677-1848

*To whom correspondence should be addressed: dwatkins@olemiss.edu

Table of Contents Pages

General Summary: Reagents and solvents were purchased from commercial sources and used without further purification unless otherwise specified. DMF were degassed in 20 L drums and passed through two sequential purification columns (activated alumina; molecular sieves for DMF) under a positive argon atmosphere. Thin layer chromatography (TLC) was performed on SiO2-60 F254 aluminum plates with visualization by UV light or staining. Flash column chromatography was performed using Purasil SiO2-60, 230–400 mesh from Fisher. 1 H NMR spectra were recorded on a Bruker Avance-300 (300 MHz), Bruker Avance DRX-500 (500 MHz spectrometer and are reported in ppm using solvent as an internal standard (CDCl 3 at 7.26 ppm). Data reported as: s = singlet, d = doublet, t = triplet, q = quartet, p = pentet, m = multiplet, b = broad, ap = apparent; coupling constant(s) in Hz; integration.

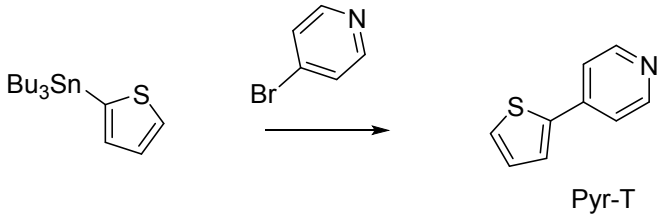

Scheme S1. Synthesis of **Pyr-T**

Preparation of the XB acceptor, **Pyr-T,** primarily followed literature preparation of similar derivatives. The XB compound, **Pyr-T,** was synthesized via Stille cross-coupling in one step in an overall yields of 93.2 %. For the preparation of co-crystals, **Pyr-T** were dissolved separately in THF with iodopentafluorobenzene in borosilicate glass vials. The resulting mixture was treated with ultrasonic waves for 10 minutes. The open vials were closed in a secondary vial containing *n*-hexane. The solvent was allowed to evaporate at -20 ^{o}C for a 14 days until the formation of crystals.

Pyr-T (1). To a 25 mL two-necked round-bottom flask was added 4-bromopyridine hydrochloride (0.50 g, 2.56 mmol) and tetrakis(triphenylphosphine) palladium (0) (0.44 g, 0.38 mmol) under argon. Anhydrous DMF (10 mL) and triethylamine (0.29 g, 2.82 mmol) were injected in with stirring. After stirred for 30 minutes, 2-(tributylstannyl) thiophene (1.00 mL, 3.08 mmol) was injected and the mixture was heated to 100 ^{o}C and stirred for 18 hours. The reaction was quenched with 1M NaOH solution to adjust the pH=8. Then extracted with methylene chloride and the organic layers were combined, dried over anhydrous Na_2SO_4, filtered and evaporated under reduced pressure. The residue was purified by column chromatography on silica gel (ethyl acetate/hexane, 70 % EA) to give a white solid with a yield of (384 mg) 93.2%. ^{1}H NMR: (300 MHz, DMSO-d6) ppm δ 8.57, 7.81, 7.74, 7.64, 7.22. The ^{1}H NMR data match that found in the literature.[1]

Solution-based NMR studies (150 mM in toluene-d_8)

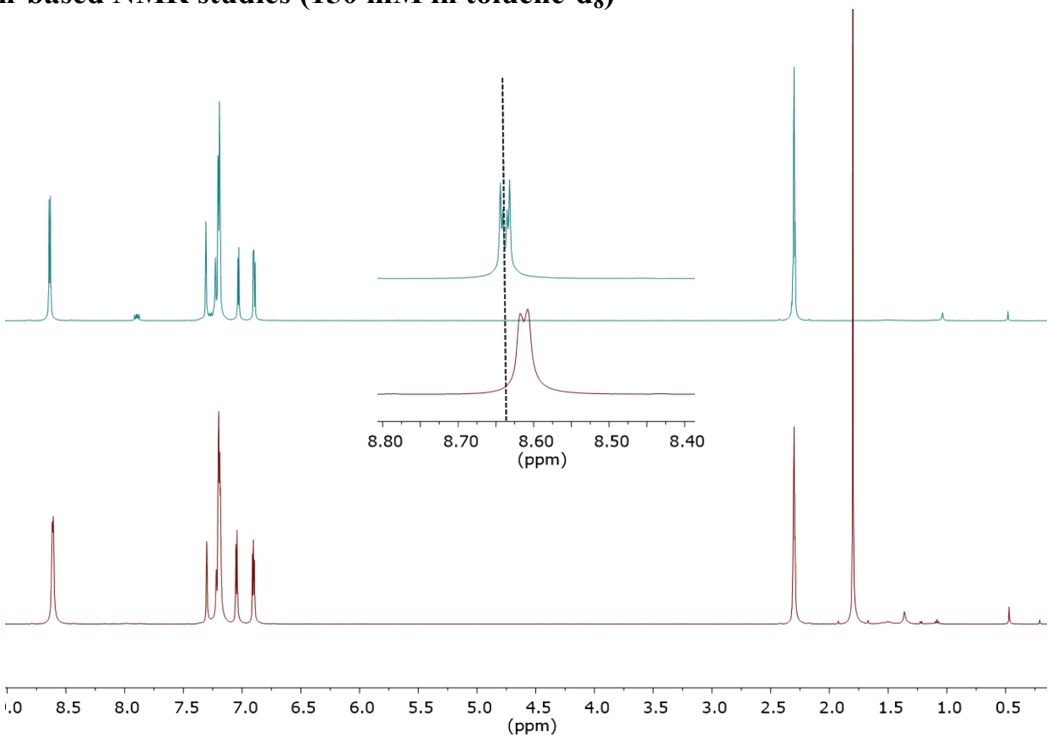

Figure S1. 1H NMR results comparing **Pyr-T**(blue) and co-complex of **Pyr-T:IPFB** (red).

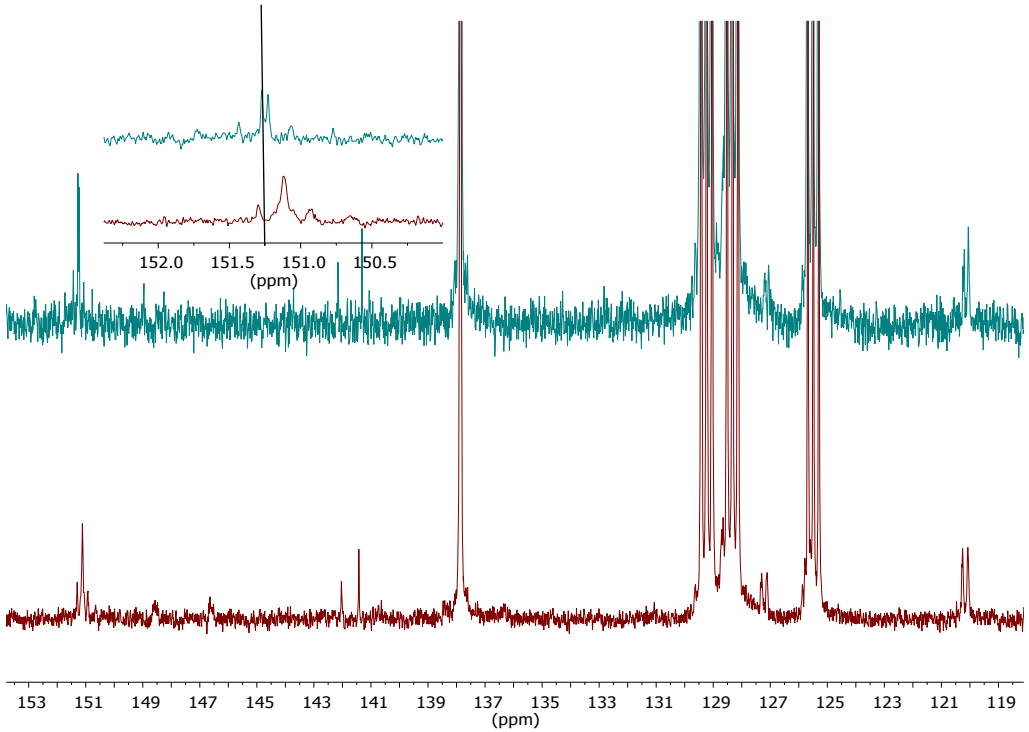

Figure S2. 13C NMR results comparing **Pyr-T** (blue) and co-complex of **Pyr-T:IPFB** (red)

Computational Detail

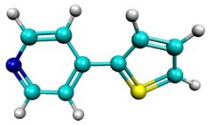

Figure S3. Optimized structure of the **Pyr-T** monomer

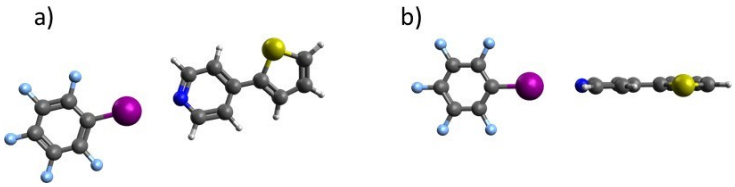

Figure S4. Optimized structures: a) co-planar minimum (C_1); b) perpendicular transition state (C_s)

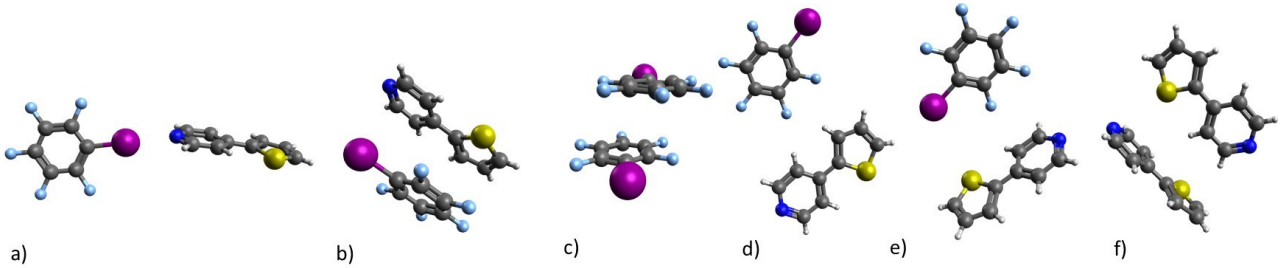

Figure S5. Nearest-neighbor pairwise contacts in crystal structure and averaged energy of interaction: a) halogen bonded (XB) -7.2 kcal/mol; b) slipped stacking -8.6 kcal/mol; c) edge-to-edge (E to E) -1.1 kcal/mol; and d) face-to-edge (F to E) -0.7 kcal/mol

Table S1. Summary of contact energetics observed in the crystal structure

Eint	**M06-2X/PopleTZ + ECP**		**M06-2X/Def2-TZVPD**		**M06-2X/aug-cc-pVTZ-pp**		**Average**
(kcal/mol)	no-CP	CP	no-CP	CP	no-CP	CP	
XB	-7.7	-7.4	-7.0	-6.9	-7.1	-6.9	-7.2
Slipped Stack	-10.0	-8.3	-8.4	-7.8	-9.0	-8.0	-8.6
Stacked $(IPFB)_2$	-7.4	-5.2	-5.8	-5.1	-6.5	-5.2	-5.8
E to E	-1.5	-1.0	-1.1	-0.9	-1.3	-1.0	-1.1
F to E	-1.1	-0.6	-0.7	-0.5	-0.9	-0.6	-0.7
F to E $(Pyr\text{-}T)_2$	-4.9	-4.2	-4.4	-4.0	-4.5	-4.1	-4.4

CP = Boys-Bernardi counterpoise procedure

PopleTZ+ECP = 6-311++G(2df,2pd) basis set for all atoms except I (LANLDZ for I atom)

Spectroscopic Analysis Raman Spectroscopy

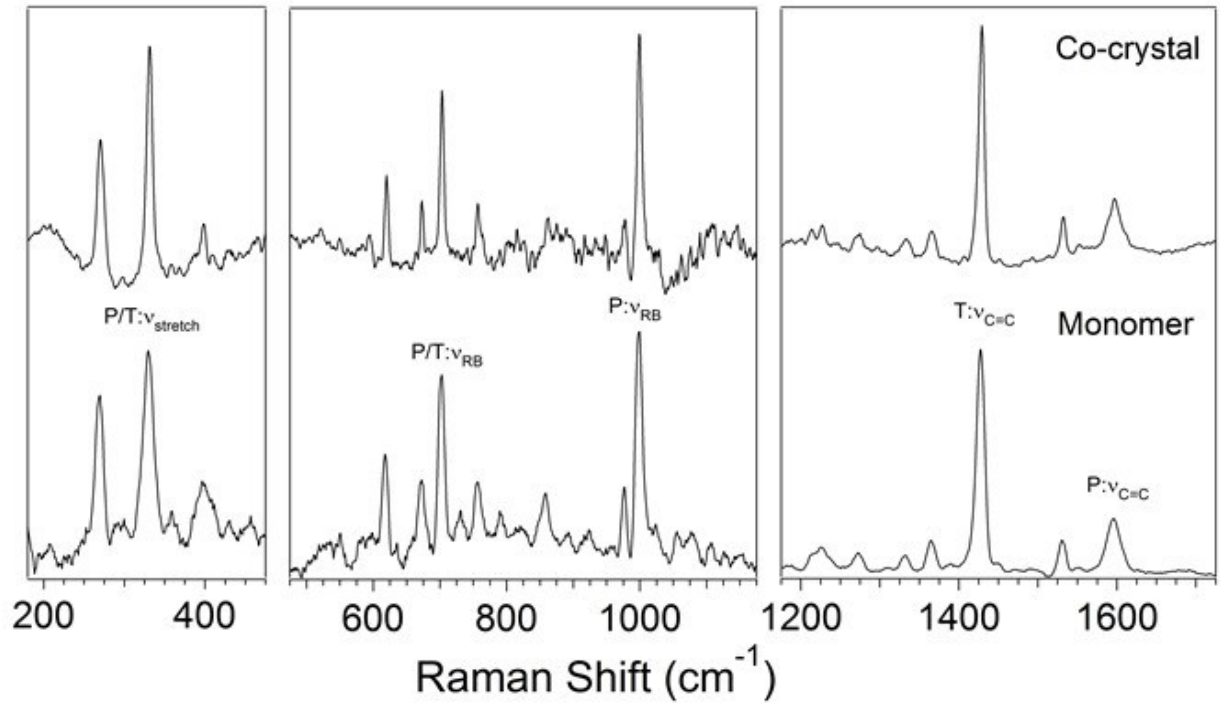

Figure S6. Vibrational energy shifts were observed when comparing the experimental Raman spectrum of neat **Pyr-T** and **Pyr-T** within the co-crystal.

Table S2. Summary of selected vibrational frequencies (cm^{-1}) for **Pyr-T** and complexes with iodopentafluorobenzene;*M062X/def2-TZVPD

Pyr-T Peak Location	Co-Crystal Peak Location	Experimental Shift	Theoretical Shift**
270	270	0	+4
330	331	+1	+7
397	398	+1	+3
618	620	+2	+4
671	673	+2	-2
703	703	0	+4
757	757	0	-1
999	1000	+1	+6
1332	1333	+1	1
1365	1366	+1	-4
1428	1429	+1	-1
1531	1532	+1	+2
1596	1597	+1	+1

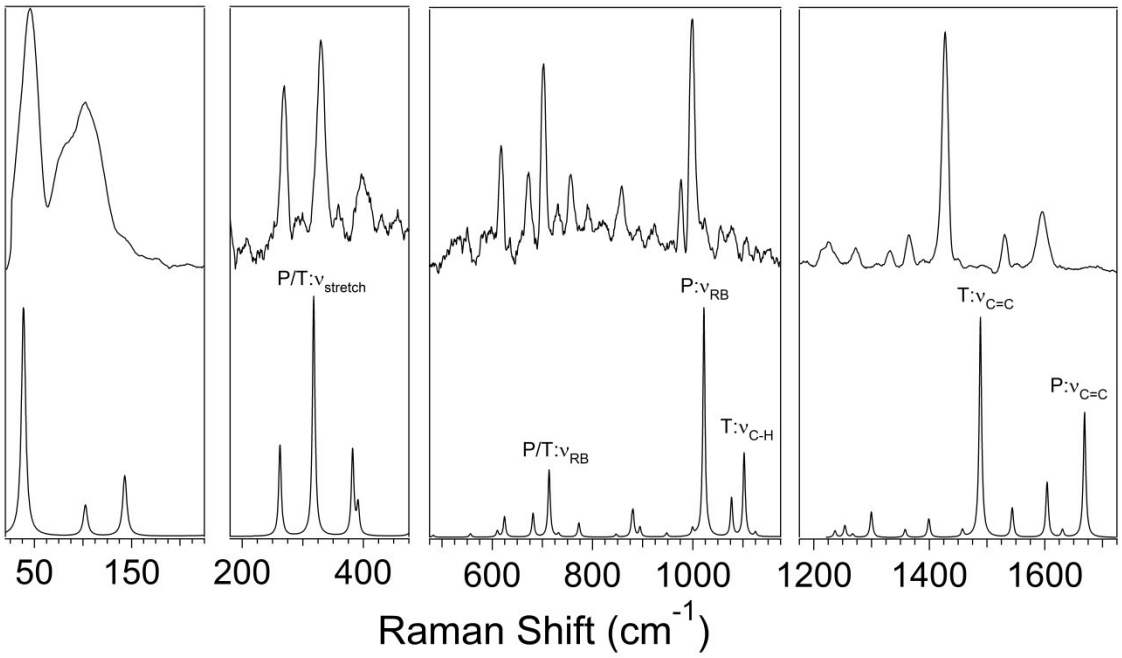

Figure S7. Comparison of the experimental (top) and theoretical (bottom, using the M06-2X/aug-cc-pVTZ method and basis set combination) Raman spectra of **Pyr-T**.

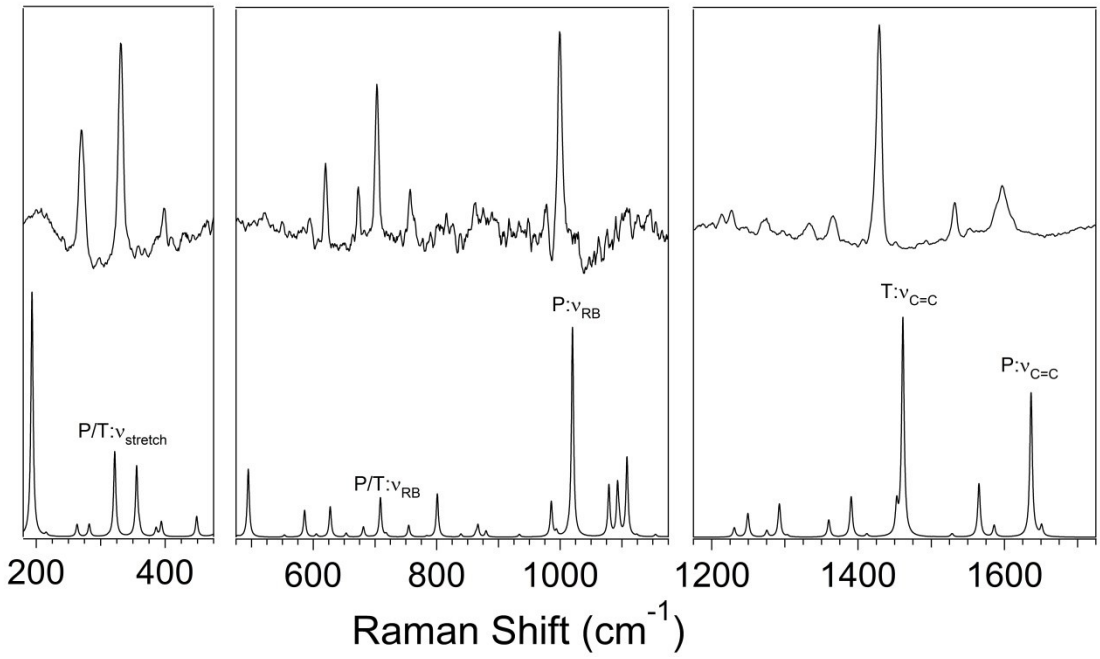

Figure S8. Comparison of the experimental (top) and theoretical (bottom, using the B3LYP/6-311++G(*2df*,*2pd*) method and basis set combination) Raman spectra of **Pyr- T** within the co-crystal.

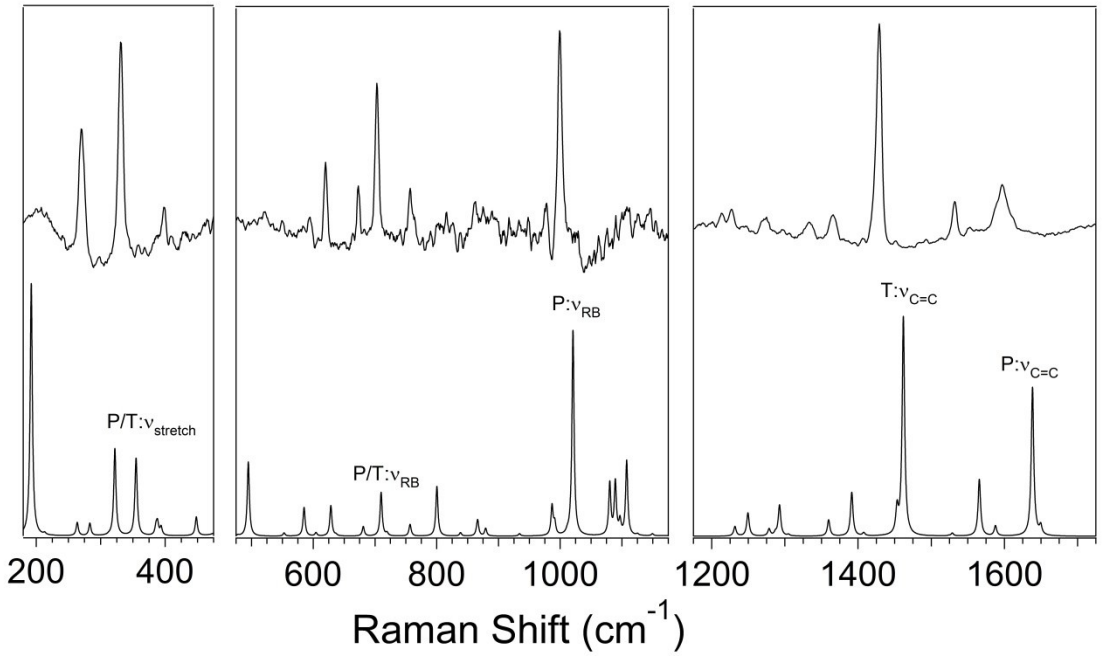

Figure S9. Comparison of the experimental (top) and theoretical (bottom, using the B3LYP/Def2-TZVPD method and basis set combination) Raman spectra of **Pyr-T** within the co-crystal.

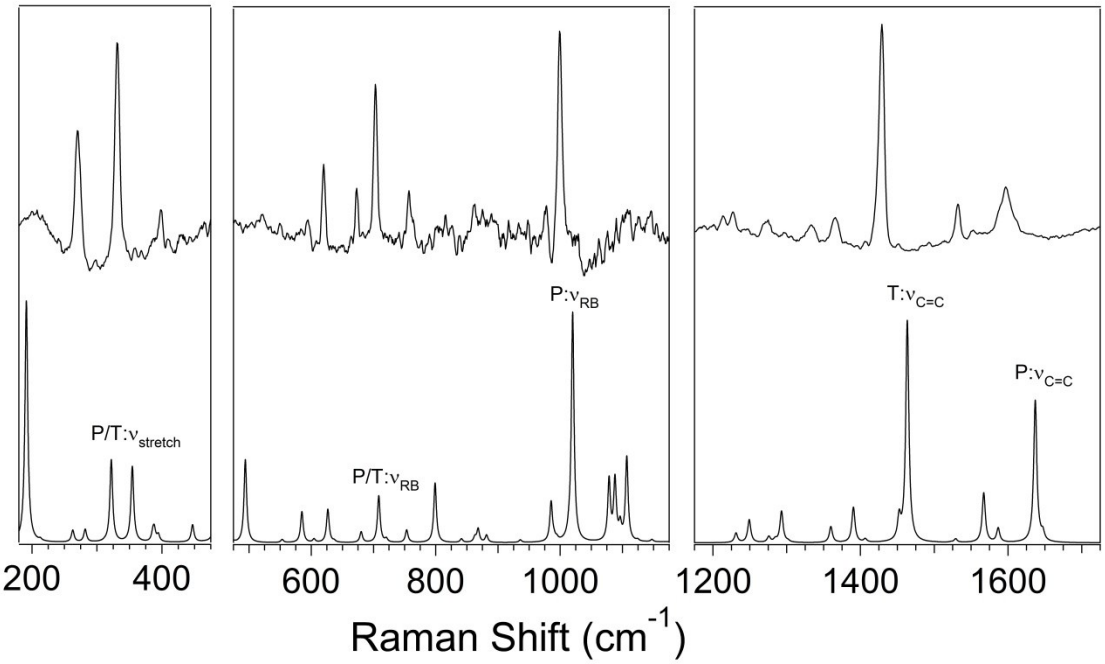

Figure S10. Comparison of the experimental (top) and theoretical (bottom, using the B3LYP/aug-cc-pVTZ method and basis set combination) Raman spectra of **Pyr-T** within the co-crystal.

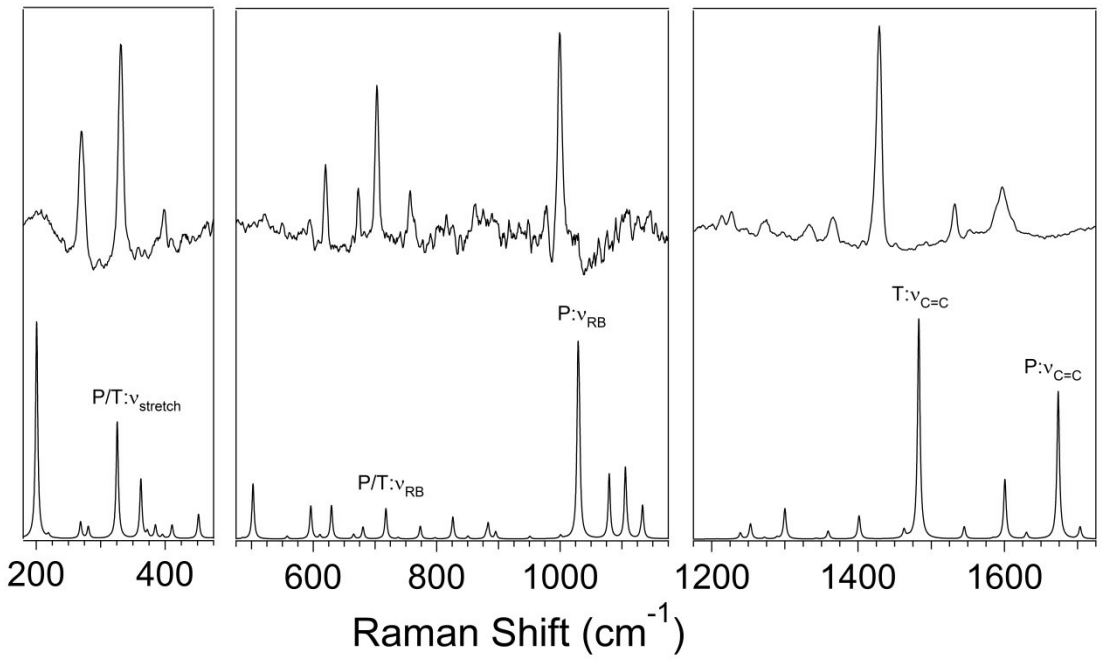

Figure S11. Comparison of the experimental (top) and theoretical using the M06-2X/6-311++G(2*df*,2*pd*) method and basis set combination (bottom) Raman spectra of **Pyr- T**.

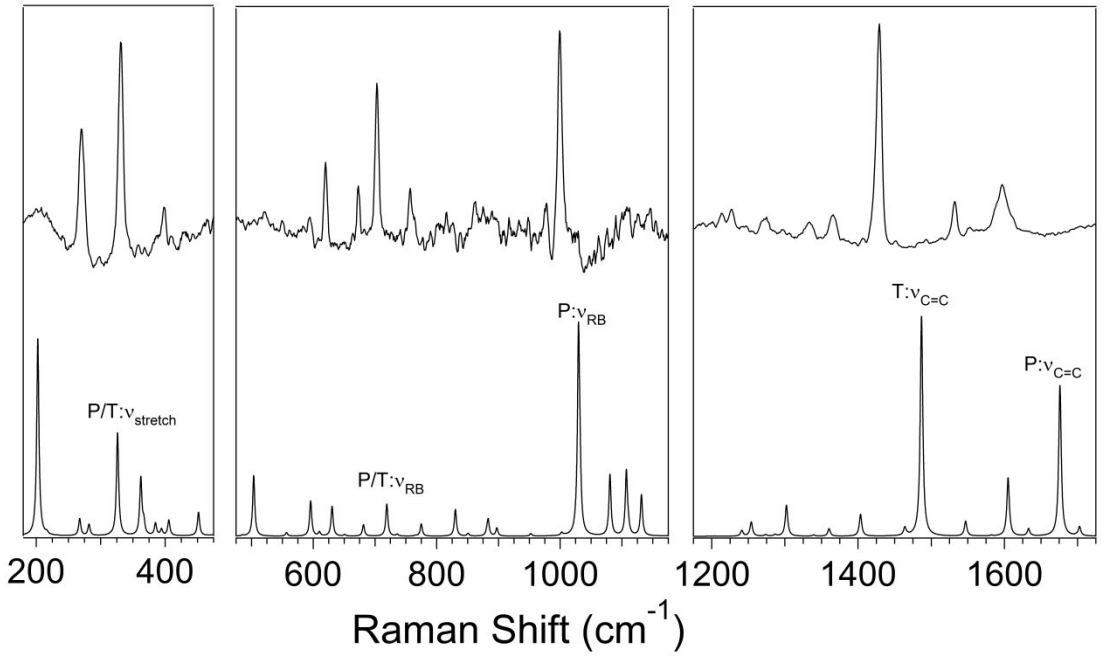

Figure S12. Comparison of the experimental (top) and theoretical using the M06-2X/Def2-TZVPD method and basis set combination (bottom) Raman spectra of **Pyr- T**

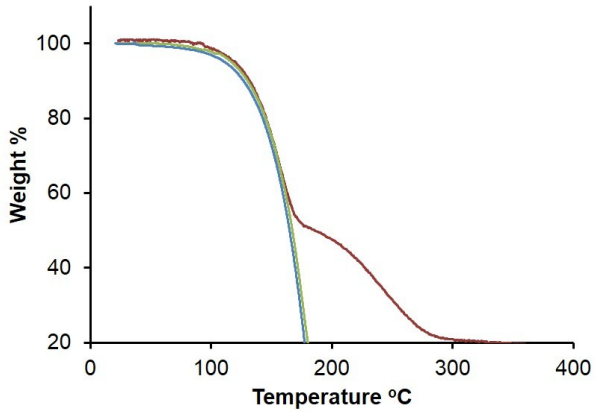

Figure S13. Thermogravimetric analysis of **Pyr-T** (green) and the co-crystal (red) indicate a ~ 60 °C higher decomposition temperature for the supramolecular assembly as well as a dual step decomposition. The dual step decomposition is due to a dissociation of one component (i.e. Pyr-T) from the assembly prior to decomposition of the entire supramolecular structure.

Table 3. Crystal data and structure refinement for Pyr-T_IPFB.

Identification code	shelxl	
Empirical formula	C15 H7 F5 I N S	
Formula weight	455.18	
Temperature	100(2) K	
Wavelength	0.71073 Å	
Crystal system	Monoclinic	
Space group	P2(1)/n	
Unit cell dimensions	a = 8.7694(5) Å	□= 90°.
	b = 7.5097(4) Å	□= 91.757(3)°.
	c = 22.9574(13) Å	□ = 90°.
Volume	1511.16(15) $Å^3$	
Z	4	
Density (calculated)	2.001 Mg/m^3	
Absorption coefficient	2.307 mm^{-1}	
F(000)	872	
Crystal size	0.32 x 0.16 x 0.12 mm^3	
Theta range for data collection	1.77 to 26.49°.	
Index ranges	-11<=h<=11, -9<=k<=9, -28<=l<=28	
Reflections collected	26339	
Independent reflections	3130 [R(int) = 0.0266]	

Completeness to theta = 25.00°	100.0 %
Absorption correction	Semi-empirical from equivalents
Max. and min. transmission	0.7693 and 0.5256
Refinement method	Full-matrix least-squares on F^2
Data / restraints / parameters	3130 / 0 / 209
Goodness-of-fit on F^2	1.146
Final R indices [I>2sigma(I)]	R1 = 0.0158, wR2 = 0.0371
R indices (all data)	R1 = 0.0171, wR2 = 0.0377
Largest diff. peak and hole	0.394 and -0.436 e.Å^{-3}

References

(1) Constable, E. C.; Housecroft, C. E.; Neuburger, M.; Schmitt, C. X. *Polyhedron* **2006**, *25*, 1844.